FISEVIER

Contents lists available at ScienceDirect

Ocean Engineering

journal homepage: www.elsevier.com/locate/oceaneng



On the stability of a free-to-rotate short-tail fairing and a splitter plate as suppressors of vortex-induced vibration



Gustavo R.S. Assi ^{a,*}, Peter W. Bearman ^b, Michael A. Tognarelli ^c

- ^a Dept. of Naval Arch. and Ocean Eng., University of São Paulo, São Paulo, Brazil
- ^b Department of Aeronautics, Imperial College, London, UK
- ^c BP America Production Company, Houston, USA

ARTICLE INFO

Article history: Received 10 December 2013 Accepted 20 October 2014 Available online 6 November 2014

Keywords: Vortex-induced vibration Galloping Suppression Splitter plate Short-tail fairing Offshore risers

ABSTRACT

Experiments in the Reynolds number range of 1000 to 12,000 have been carried out on a free-to-rotate short-tail fairing fitted to a rigid length of circular cylinder to investigate the effect of rotational friction on the stability of this type of VIV suppressor. Measurements of the dynamic response are presented for models with low mass and damping which are free to respond in the cross-flow and streamwise directions. It is shown how vortex-induced vibration can be reduced if the rotational friction between the cylinder and the short-tail fairing exceeds a critical limit. In this configuration the fairing finds a stable position deflected from the flow direction and a steady lift force appears towards the side to which the fairing has deflected. The fluid-dynamic mechanism is very similar to that observed for a free-to-rotate splitter plate of equivalent length. A non-rotating fairing as well as splitter plates is shown to develop severe galloping instabilities in 1-dof experiments.

© 2014 Elsevier Ltd. All rights reserved.

1. Introduction

Efficient suppression of flow-induced vibration (FIV) of slender submarine structures is a challenging and interesting problem for the offshore industry and the scientific community. Various methods for suppressing vortex-induced vibrations (VIV) of bluff bodies have been investigated over the past decades. With the advancement of offshore oil exploration, research on VIV suppressors was pushed to a new level. The industry demands suppressors that are not only efficient for low mass-damping systems but also that could be installed under harsh environmental conditions; such is the case for offshore risers. Zdravkovich (1981) and Every et al. (1982) present comprehensive reviews of solutions varying from the simple attachment of ribbons to quite expensive devices such as helical strakes and fairings. Drilling risers may typically be inspected more often than production risers, therefore fatigue damage is not as important a concern as the steady loads caused by strong currents. Therefore, besides suppressing FIV, suppressors must reduce drag consequently reducing pipe bend and wear risk during drilling operations.

E-mail address: g.assi@usp.br (G.R.S. Assi). URL: http://www.ndf.poli.usp.br (G.R.S. Assi).

It is known that free-to-rotate suppressors may experience hydrodynamic instabilities that will not only cause a substantial increase in drag but also prevent them from suppressing vibrations (Assi et al., 2009). Actually, an unstable free-to-rotate suppressor may induce more vigorous structural vibrations excited by a type of flutter mechanism. Assi et al. (2009) have shown that the instability of free-to-rotate suppressors is directly related to the level of rotational resistance encountered in the system as well as geometric parameters such as plate length. They performed experiments in laboratory scale and showed that a free-to-rotate suppressor formed by a single splitter plate may need a minimum rotational resistance (or be above a critical rotational friction) to enable a stable configuration with effective suppression. The same was verified for free-to-rotate suppressors composed of two parallel plates (Assi et al., 2012), revealing that a minimum rotational resistance is necessary to stabilise the devices. Assi et al. (2009, 2010a) have also shown that 1D-long parallel plates can be very efficient in suppressing both VIV and WIV (wakeinduced vibration). WIV occurs when the downstream body of a set is excited by the unsteady wake generated from another body placed upstream (Assi et al., 2010b, 2013a).

In the present work we contribute to the understanding of the hydrodynamic mechanism behind a type of free-to-rotate device known as the short-tail fairing compared with a cylinder associated with a simple geometry of a splitter plate. We focus on the dynamic stability and hydrodynamic phenomena that cause the

^{*} Correspondence to: PNV Dept. Eng. Naval e Oceânica, Escola Politécnica da Universidade de São Paulo, Av. Prof Mello Moraes 2231, 05508-030 São Paulo - SP, Brazil

fairing and the splitter plate to behave in quite the same way. A parametric investigation of the geometry of suppressors, in special the splitter plate, is not the concern of the present work. For that matter, the reader may refer to other works of the same authors (Assi et al., 2012, 2013b; Assi and Franco, 2013).

2. Free-to-rotate suppressors

It is known that if vortex shedding from a fixed cylinder is eliminated, say by the use of a long splitter plate (Cimbala and Garg, 1991), then drag is reduced. Hence conceptually an effective VIV suppression device should be able to reduce drag rather than increase it. This simple idea was the motivation for the development of suppressors such as splitter plates and fairings that act primarily by disrupting the vortex shedding mechanism on the near wake of bluff bodies by delaying the interaction between the separated shear layers.

Assi et al. (2009) have shown that suppression of cross-flow and in-line VIV of a circular cylinder, with resulting drag coefficients less than that for a fixed plain cylinder, has been achieved using two-dimensional control plates in low mass-damping systems. A free-to-rotate splitter plate was also found to suppress VIV but instead of remaining aligned with the flow on the centreline of the wake the plate adopted a stable but deflected position when it was released. VIV was suppressed, throughout the range of reduced velocity investigated, and drag reduced below that of a plain cylinder. Cimbala and Garg (1991) had also observed this bi-stable behaviour for a free-to-rotate cylinder fitted with a splitter plate.

Particle-image velocimetry (PIV) measurements performed by Assi et al. (2009) showed that on the side to which the plate deflected the separating shear layer from the cylinder appeared to attach to the tip of the plate and this had the effect of stabilising the near wake flow. Vortex shedding was visible downstream but this did not feed back to cause vibrations. An unwanted effect was that a steady transverse lift force developed on the cylinder towards the side to which the splitter plate deflected. This steady lift could be eliminated by using a pair of splitter plates arranged so that the shear layers that spring from both sides of the cylinder attach to the tips of the plates. The maximum suppression and drag reduction occurred with a pair of free-to-rotate parallel plates installed on the sides of the cylinder.

Assi et al. (2009) also found that the level of rotational friction between the free-to-rotate plate and the cylinder plays a fundamentally important role, needing to be "high enough to hold the device in a stable position, while still allowing them to realign if the flow direction changes. Devices with rotational friction below a critical value oscillate themselves as the cylinder vibrates, sometimes increasing the amplitude of cylinder oscillation higher

than that for a plain cylinder". All devices with rotational friction above a critical value appeared to suppress VIV and reduce drag. However, if the rotational resistance was above a limiting threshold the suppressors could not rotate and an undesired galloping response was initiated.

In the present study we set out with the hypothesis that short-tail fairings and short splitter plates are able to suppress VIV based on the same fluid-dynamic mechanism. Short-tail fairings are not "fairings" in the strict sense of the term, meaning that they do not make a streamlined body. For this to happen the length of the fairing would have to be many times the diameter of the cylinder, as shown in Henderson (1978), Wingham (1983) and Packwood (1990). In essence, we believe a short-tail fairing acts in the near wake with fully separated flow avoiding the interaction between the shear layers and delaying vortex shedding, therefore the same mechanism as the splitter plate.

If this is true, we expect short fairings to find stable but deflected positions towards one of the sides of the cylinder instead of aligning itself with the flow. In the same manner as splitter plates, the stability of short fairings might also depend on a minimum level of rotational friction in order to suppress VIV. The effect of rotational friction on the stability of a short-tail fairing is what this present study sets out to investigate. However, if friction is too high the suppressor may not find itself free to rotate around the cylinder, but stuck with no angular movement. If this is the case, the system becomes susceptible to galloping, which may cause severe vibrations in a very different fashion from VIV.

3. Experimental arrangement

Two types of suppressors were tested in this experimental campaign: a free-to-rotate splitter plate and a short-tail fairing. Fig. 1(a) presents the geometric parameters for the splitter plate. Plate length L/D could be varied by changing the plate made out of acrylic plastic. The short-tail fairing was made of a triangular

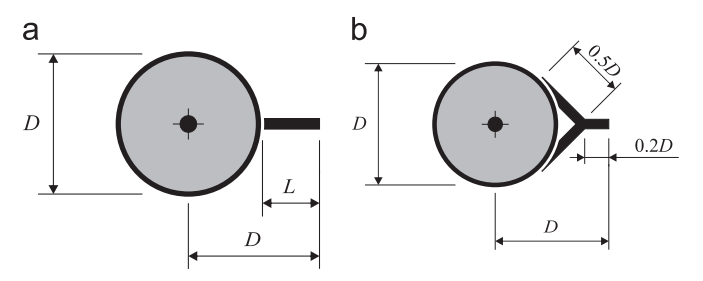


Fig. 1. Geometries for splitter plates and a short-tailed fairing. (a) Short splitter plate; (b) Short-tail fairing.

fairing with a flat tail piece as shown in Fig. 1(b). Devices with a similar geometry are used by the offshore industry following its appearance as a commercial solution to reduce VIV (Allen and Henning, 1995). The geometry adopted in this work was based on the proportions found in Pontaza and Chen (2006). It consisted of two perpendicular plates of 0.5D in length joined at the tip to a short 0.2D-long tail plate. The characteristic length of the fairing was 0.5D if measured from the base of the cylinder, thus of the same order as the $L/D\!=\!0.5$ splitter plate.

Suppressors were supported by two rotating arms at each end mounted on low-friction ball bearings. Plates were kept at a small distance from the cylinder wall in order to allow the devices to freely rotate about the centre of the cylinder. Control of the rotational friction was achieved by adjusting a screw pushing a small brake plate between the rotating parts. The same system was employed by Assi et al. (2009).

Experiments were carried out on devices fitted to a rigid length of a circular cylinder free to respond to VIV. The investigation was performed during a test campaign in 2007 in a recirculating water channel in the Department of Aeronautics, Imperial College, London. The parallel test section was 0.6 m wide, 0.7 m deep and 8.0 m long. The flow speed U was continuously variable and good quality flow could be obtained up to at least 0.6 m/s. The cylinder model was constructed from 50 mm diameter acrylic tube, giving a maximum Reynolds number of approximately 30,000, based on cylinder diameter D.

Models could be mounted in two different elastic rigs, one that allowed one-degree-of-freedom (1-dof) motion in the cross-flow direction and another that allowed two-degrees-of-freedom (2-dof) motion in the cross-flow and streamwise directions. The 2-dof rig allowed for motion that is closer to the real application of suppressors in offshore risers, hence most of the results discussed in the present study were obtained from experiments in this rig. Also, 2-dof experiments proved to be rather important to evaluate the stability of free-to-rotate suppressors due to the effect of streamwise movement over the rotation of the plates. Of course the rotation of the plate could be thought of as a third dof in the dynamic system, but in the present work we shall only consider the response of the cylinder in the cross-flow and streamwise directions.

For the 2-dof experiments, models were mounted on a very low damping rig shown in Fig. 2. The cylinder model was mounted at the lower end of a long carbon fibre tube which formed the arm of a rigid pendulum. The top end of the arm was connected to a universal joint fixed at the ceiling of the laboratory so that the cylinder model was free to oscillate in any direction in a pendulum motion.

The cylinder was vertically aligned at the centre of the test section, distant 300 mm from each of the side walls. A total blockage of 8.3% was judged not to affect the overall response based on the study of Brankovic (2004). A small gap of 2 mm was left between the bottom end of the cylinder and the floor. Also

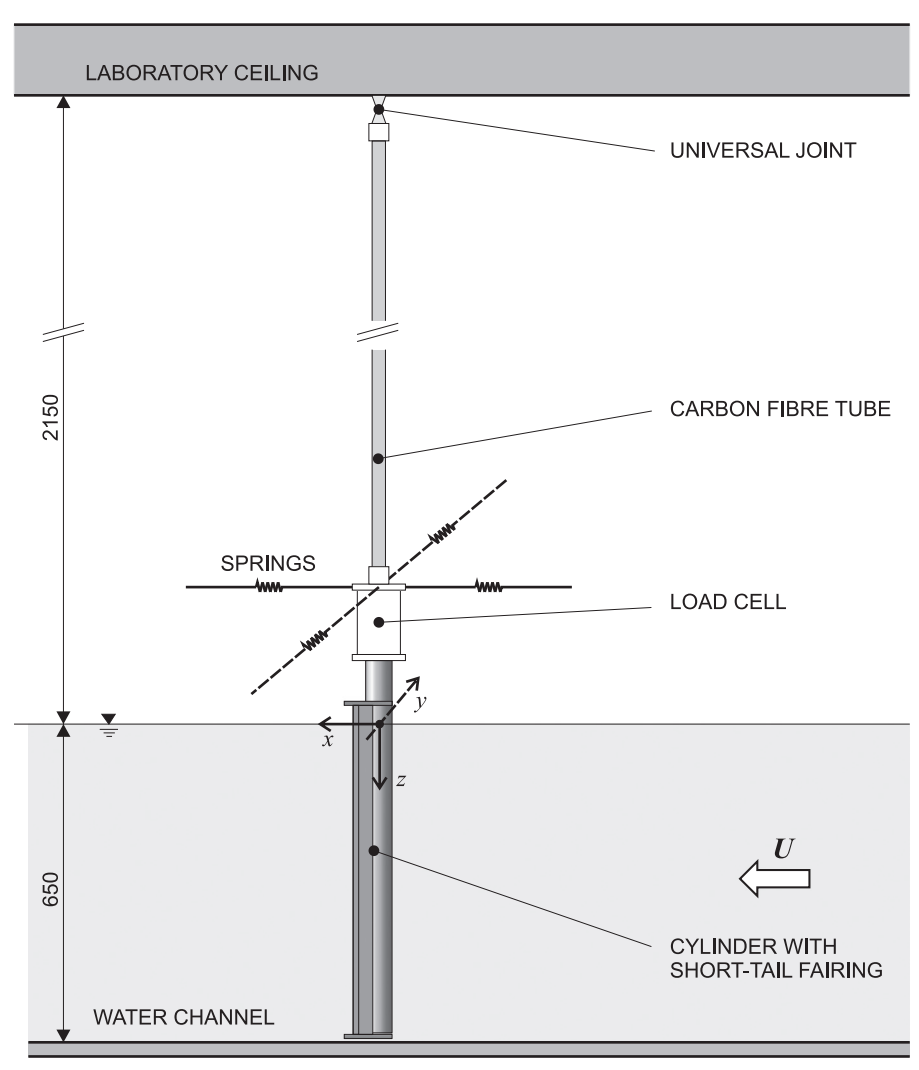


Fig. 2. Representation of the cylinder with a short-tail fairing mounted on the 2-dof rig in the test section of the water channel. Dimensions are in millimetres.

based on previous studies employing the same set-up (Assi et al., 2009, 2010b, for example), the different end conditions at the free surface and the bottom of the cylinder did not affect the overall behaviour of the system as far as flow-induced vibration is concerned.

Two independent optical sensors were employed to measure displacements in the x- and y-directions at the mid-length of the model. It should be noted that for a displacement equal to 1 diameter the inclination angle of the cylinder was only just over 1° from the vertical. Two pairs of springs were installed in the x- and y-axes to set the natural frequencies in both directions of motion allowing different natural frequencies to be set for each direction.

Although the cylinder was initially aligned in the vertical position, in flowing water the mean drag displaces the cylinder from its original location. To counteract this effect, both pairs of springs were attached to a frame that could be moved back and forth in the direction of the flow. For each flow speed there was a position of the frame that maintained the mean position of the cylinder in the vertical alignment. By using two pairs of springs perpendicular to each other, the assembly has nonlinear spring constants in the transverse and in-line directions for large displacements. Movement in the transverse direction will cause a lateral spring deflection in the in-line direction and vice versa. This nonlinearity is minimised by making the springs as long as possible, hence the in-line springs were installed at the end of 4 m-long wires, fixed at the extremities of the frame.

It is known that during the cycle of vortex shedding from bluff bodies the fluctuation of drag has double the frequency of the fluctuation of lift. Hence a particularly severe vibration might be expected to occur if the hydrodynamic forces in both directions could be in resonance with both in-line and transverse natural frequencies at the same time. For this reason, we set the streamwise natural frequency (f_{0_x}) to be close to twice the cross-flow frequency (f_{0_y}) or simply f_0) by adjusting the stiffness of both pairs of springs. The structural damping of the 2-dof rig was ζ =0.3% (measured in air), defined as a fraction of critical damping, practically the same for both principal directions of motion. A load cell was attached between the cylinder and the support system to deduce the instantaneous and time-averaged hydrodynamic forces on the cylinder model. The mass ratio m^* , defined

Table 1 Structural properties.

Model	m*	ζ (%)	<i>m</i> *ζ	f_{0_x}/f_{0_y}
Plain cylinder Splitter plate $L/D = 0.5$	1.6	0.3	0.0047	1.93
	1.7	0.3	0.0051	1.90
Splitter plate $L/D = 1.0$	1.7	0.3	0.0051	1.90
Short-tail fairing	1.7	0.3	0.0051	1.90

as vibrating mass divided by the displaced mass of water, was kept to the lowest possible value. Preliminary tests have been performed with a plain cylinder to serve as reference for comparison. Table 1 presents the structural parameters for the arrangements of cylinder and suppression device tested.

Measurements were made using a fixed set of springs and the reduced velocity range covered was from 1.5 to 13, where reduced velocity (U/Df_0) is defined using the cylinder natural frequency of oscillation in the cross-flow direction measured in air. The only flow variable changed during the course of the experiments was the flow velocity U, which, as for full-scale risers, alters both the reduced velocity and the Reynolds number. Throughout the study, cylinder displacement amplitudes (\hat{x}/D) for streamwise and \hat{y}/D for cross-flow) were found by measuring the root mean square value of response and multiplying by the square root of 2 (the so called harmonic amplitude). This is likely to give an underestimation of maximum peak response but was judged to be perfectly acceptable for assessing the effectiveness of VIV suppression devices. Displacements were nondimensionalised by dividing by the plain cylinder diameter D.

The 1-dof rig has been employed for several VIV experiments and is described in detail in Assi et al. (2010a). For brevity, we will limit ourselves to comment that the 1-dof rig consisted of a rigid support table, mounted on two carbon fibre tubes, sliding through air bearings in the cross-flow direction. Restoration was achieved by one pair of coil springs. Mass and damping were also kept to a minimum, resulting in $m^* \approx 2.6$ and $\zeta = 0.7\%$ (with a combined parameter $m^*\zeta \approx 0.0182$) for all the 1-dof experiments. The 1-dof rig was only employed for experiments in which the suppressors were not free to rotate, as will be presented below.

4. Results and discussion

Preliminary experiments performed with a plain cylinder (previously presented in Assi et al., 2009) will serve as reference for the discussion that follows. Fig. 3 presents the typical trajectories of motion for a single cylinder under 2-dof VIV in which f_{0_x} is almost twice as f_{0_v} . The x-axis for displacement is not shown in Fig. 3 for clarity, but it has the same scale as the y axis. As reduced velocity is increased, vibrations start to build up in a 'C' shape, then changing into '8'-shaped curves until the end of the synchronisation range at around reduced velocity 12. The overall response was found to be in good agreement with results from Jauvtis and Williamson (2004) (even though they had $f_{0x} = f_{0y}$) and Dahl et al. (2006). Figs. 4 and 5 both repeat the same 2-dof response for a plain cylinder projected in the cross-flow (\hat{y}/D) and streamwise (\hat{x}/D) directions, revealing a different behaviour from the typical cross-flow VIV response in 1-dof. Initial, upper and lower branches are not clearly identified but instead 2-dof vibrations build up in the form of a single branch during the synchronisation range.

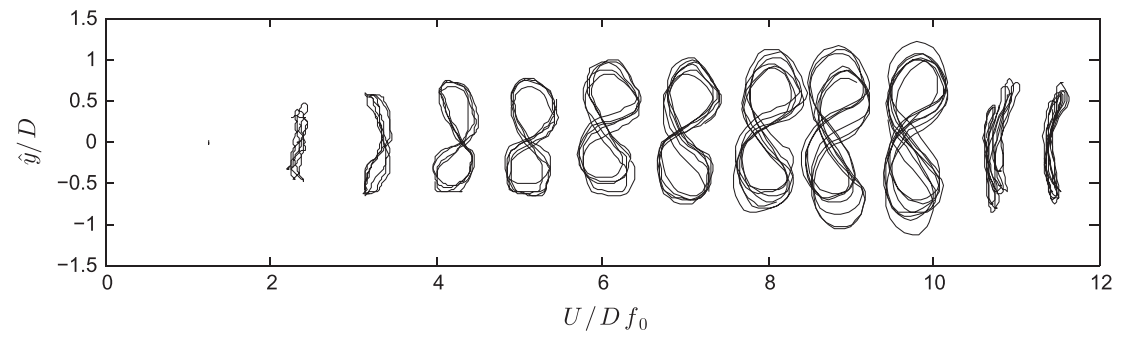


Fig. 3. Trajectories of motion for a plain cylinder.

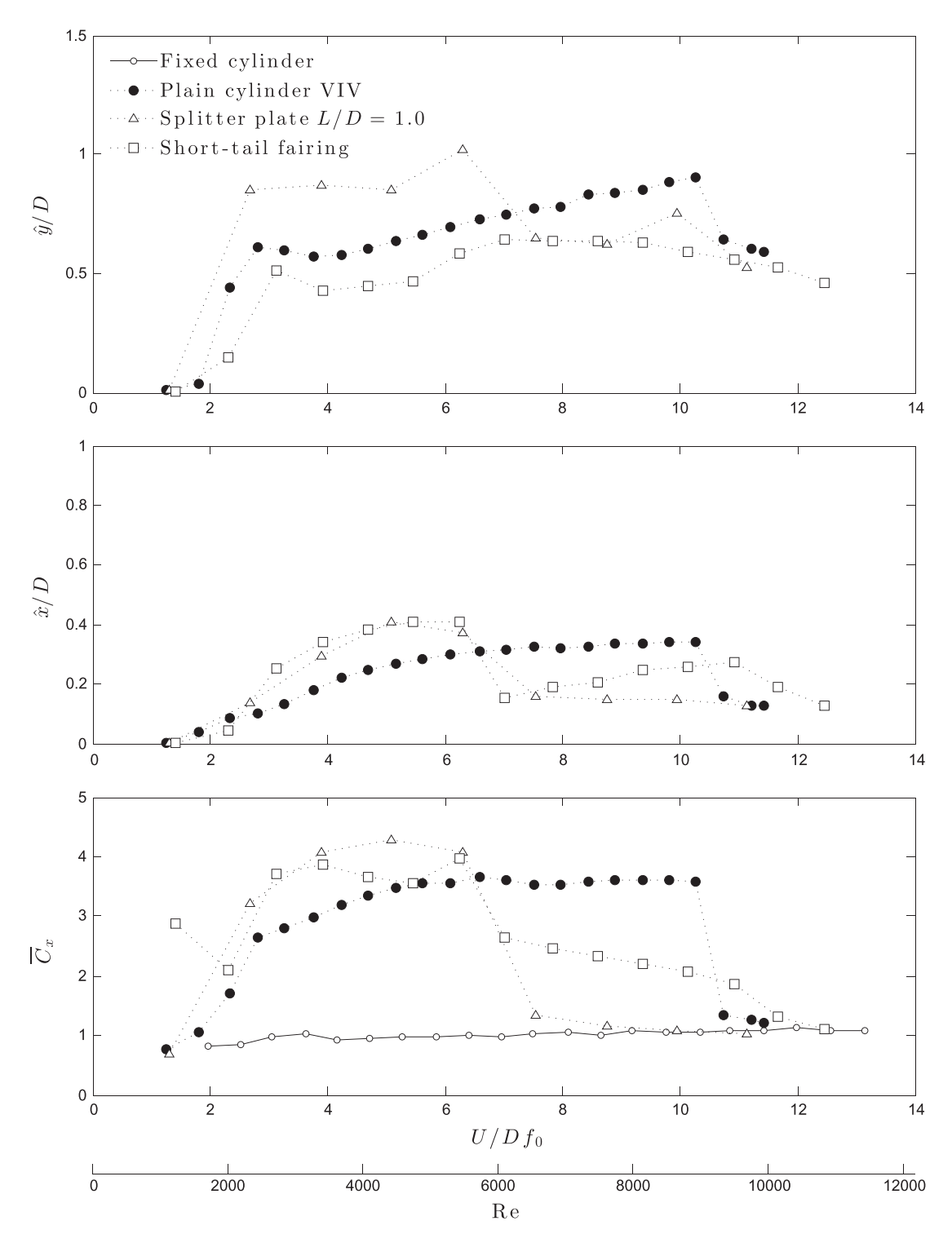


Fig. 4. 2-dof response of cylinder fitted with free-to-rotate devices with low friction ($\tau_f = 0.009 \text{ Nm/m}$). Displacement (*top*) and frequency (*middle*) of vibration and mean drag coefficient (*bottom*) versus reduced velocity.

4.1. Free-to-rotate suppressors in 2-dof

In order to investigate the rotation stability of free-to-rotate splitter plates and short-tail fairings models were prepared with two values of rotational friction τ_f . Low friction ($\tau_f = 0.009 \text{ Nm/m}$) and a high friction ($\tau_f = 0.035 \text{ Nm/m}$) cases were chosen based on the results obtained for a splitter plate presented in Assi et al. (2009). In that same paper, τ_f was measured in torque per unit length and could be rewritten as a non-dimensional friction torque

parameter

$$\tau_f^* = \frac{\tau_f}{\rho U^2 D^2},\tag{1}$$

which represents the ratio of structural torsional resistance to a hydrodynamic torque, thus varying with flow speed squared.

Similar to what was observed for a splitter plate in Assi et al. (2009), neither the splitter plate (L/D=1.0) nor the short-tail fairing with low friction ($\tau_f=0.009~{\rm Nm/m}$) came to a stable

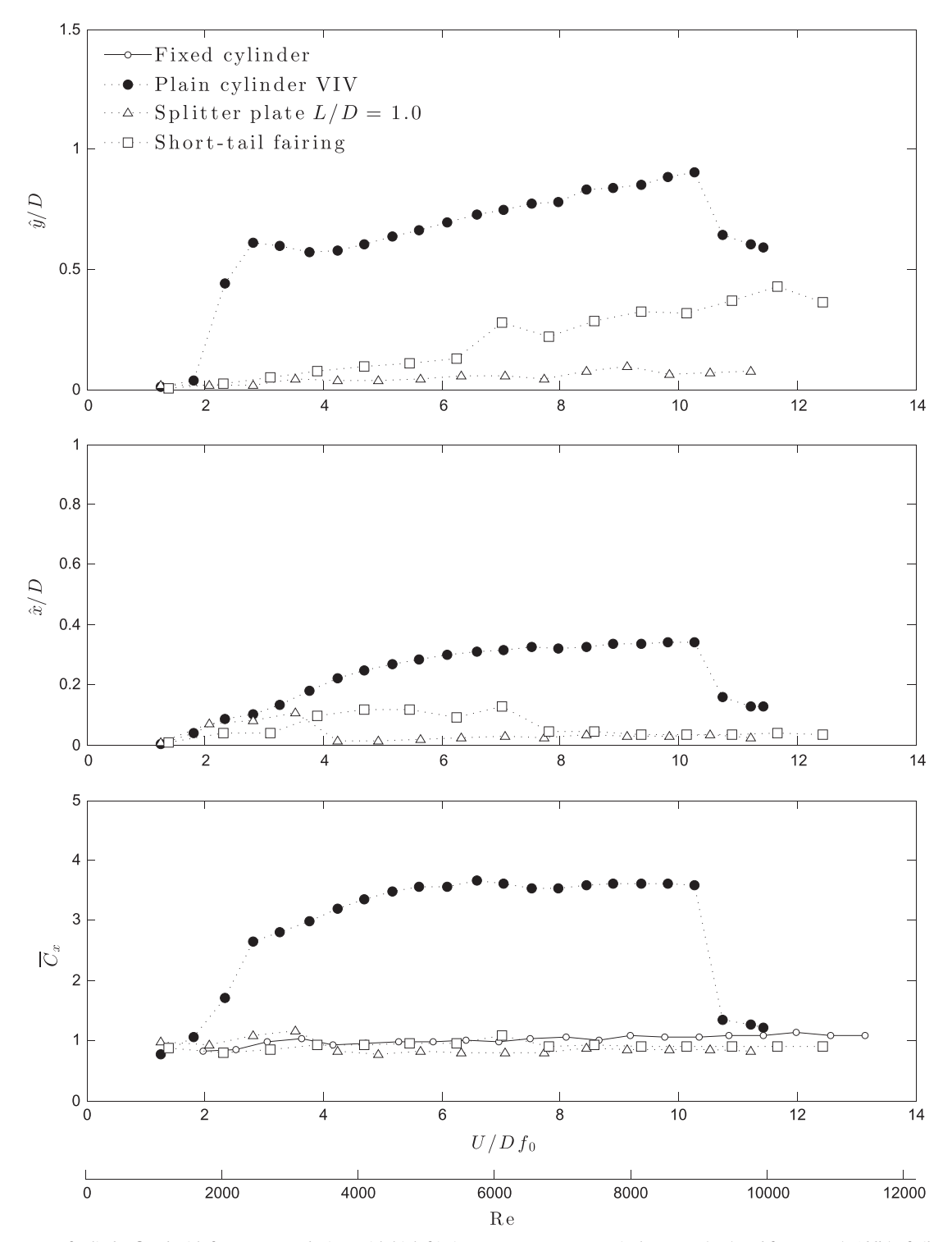


Fig. 5. 2-dof response of cylinder fitted with free-to-rotate devices with high friction ($\tau_f = 0.035 \text{ Nm/m}$). Displacement (top) and frequency (middle) of vibration and mean drag coefficient (bottom) versus reduced velocity.

angular position about the centre of the cylinder wake, instead they oscillated from side to side as the cylinder responded with VIV. The trajectories of motion presented in Figs. 6(a) and 7(a) also resemble a deformed '8' shape with amplitudes of vibration almost as high as those observed for a plain cylinder (Fig. 3) for the whole range of reduced velocities.

This effect can also be seen in Fig. 4 for cross-flow and streamwise directions in contrast with the response of the single cylinder. It reveals that while the cross-flow response of the short-tail fairing falls just below the curve for the single cylinder, the

1.0D-long splitter plate actually enhances vibration. One has to bear in mind that the characteristic length of this specific splitter plate is twice that of the short-tail fairing, thus inducing more severe oscillations when the device rotates. Streamwise responses are rather similar to both suppressors.

In contrast, both the splitter plate and the short-tail fairing presented a distinct behaviour when rotational friction was increased from $\tau_f = 0.009 \, \text{Nm/m}$ to $0.035 \, \text{Nm/m}$, as shown in Figs. 6 and 7. Both devices came to a stable position at a deflected angle (which was different for each suppressor) about the axis of

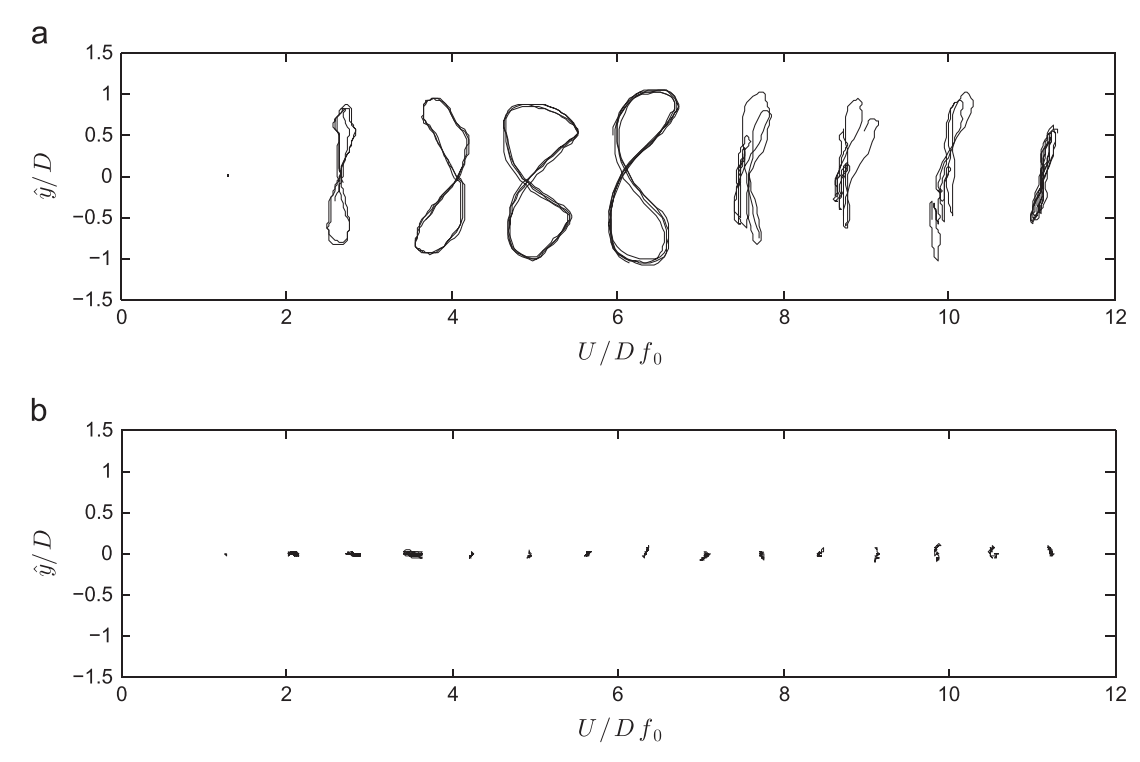
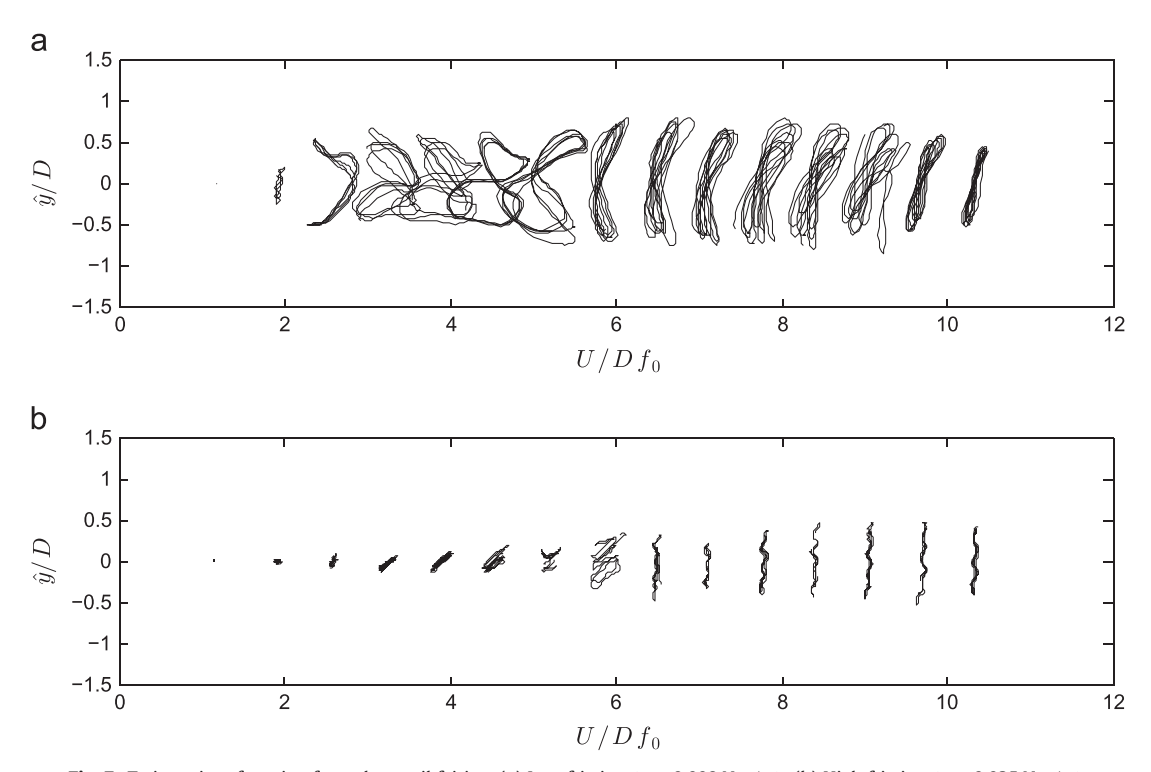


Fig. 6. Trajectories of motion for a splitter plate with L/D = 1.0. (a) Low friction ($\tau_f = 0.009 \text{ Nm/m}$); (b) High friction ($\tau_f = 0.035 \text{ Nm/m}$).



 $\textbf{Fig. 7.} \ \ \text{Trajectories of motion for a short-tail fairing. (a) Low friction } \\ (\tau_f = 0.009 \ Nm/m); \ (b) \ High \ friction \ (\tau_f = 0.035 \ Nm/m). \\$

the cylinder and, similar to what was observed for the splitter plate in Assi et al. (2009), VIV was reduced. In this angular configuration the short-tail fairing was successful in suppressing VIV, though not completely.

Fig. 5 shows that the maximum amplitude of vibration was $\hat{y}/D \approx 0.45$ in the cross-flow and $\hat{x}/D \approx 0.15$ in the streamwise directions within the synchronisation range. Significant vibration might still appear for higher reduced velocities because the fairing is not long enough to sufficiently delay the interaction of the shear

layers downstream of the body, thus vortices are feeding back and exciting the cylinder. The 1.0D-long splitter plate, on the other hand, seems to be playing this role rather well. Cross-flow and streamwise vibrations are considerably reduced and kept to a minimum through the whole range of reduced velocities investigated.

As far as drag reduction is concerned, Fig. 4 shows that both suppressors with low rotational friction presented drag coefficients higher than that of a plain cylinder under VIV for a good

part of the synchronisation range. On the other hand, once the devices were able to stabilise with high friction, the level of drag dropped to values comparable to a static plain cylinder, as presented in Fig. 5, with the 1.0D-long splitter plate being the most efficient in terms of drag reduction. The short-tail fairing did not show such as large a drag reduction as the splitter plate or other devices studied in Assi et al. (2009), but achieved an average reduction of 6% compared to a fixed cylinder if the whole range of reduced velocity (or Reynolds number) is considered.

A stable angle of deflection δ of around 25° was observed for the short-tail fairing and was very close to that found for a 0.5D-long splitter plate by Assi et al. (2009). As illustrated in Fig. 8, this angle is related to the characteristic length of the suppressor and its capacity to encounter and reattach one of the separated shear layers (Assi et al., 2009), thus we expect the short-tail fairing and a 0.5D-long splitter plate to find similar stable angular deflections.

We have observed that, likewise the splitter plate, a short-tail fairing requires a deflected position in order to stabilise and disrupt the communication between the shear layers, consequently delaying vortex shedding and suppressing VIV. However, as a consequence of this new asymmetric configuration, the fairing also generates a mean lift force towards the side to which it has deflected. In practise, long risers are fitted with a series of fairings mounted along the span of the pipe. It is possible, therefore, that some fairings might randomly deflect to one side whereas others deflect to the opposite side, in a way that the resultant lift force generated on the entire riser is neutralised. This prediction was not verified in our experiments, but operators have reported this behaviour.

4.2. Fixed suppressors in 1-dof

Now, if a deflected position is capable of generating steady lift, this lateral force might become a problem for a device that got stuck at a fixed position about the cylinder. Experiments with fixed suppressors (not free to rotate) were designed to verify this. Devices were fixed at 180° in relation to the flow direction (as shown in Fig. 1) by locking the rotating arms about the cylinder. In addition to the short-tail fairing, two splitter plates of length L/D=0.5 and 1.0 were tested in the 1-dof rig (cross-flow direction only). Responses are compared against the typical VIV response of a plain cylinder with 1-dof from Assi et al. (2010a).

As shown in Fig. 9, the response is very different from that obtained for free-to-rotate suppressors. Both splitter plates and the short-tail fairing presented a very vigorous transverse galloping oscillation that, with increasing reduced velocity, would apparently

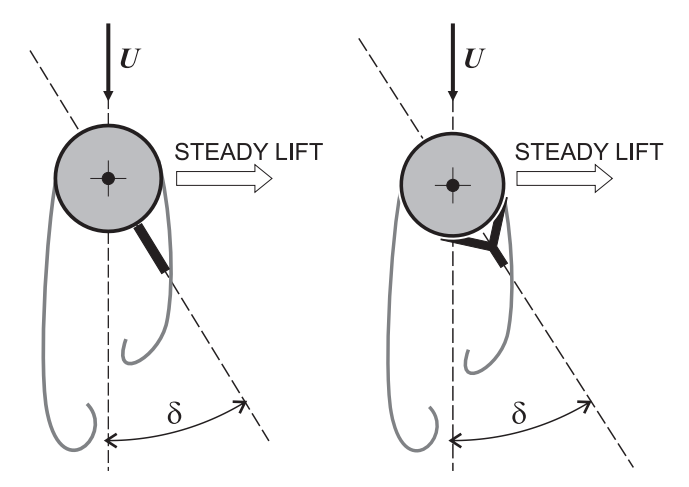


Fig. 8. Steady lift generated on the cylinder due to the deflection of the suppressors.

increase without limit. In this 1-dof experiment the maximum amplitude of the rig for cross-flow oscillation was limited to about 2D and this was reached by the splitter plates at reduced velocity of about 10. The same behaviour has been observed for the short-tail fairing in the present work. The fairing was allowed to vibrate for higher reduced velocities and the response presented an abrupt decrease in displacement at $U/Df_0 \approx 14$. Stappenbelt (2010) performed experiments with low aspect ratio cylinders fitted with splitter plates with $L/D \leq 4$ and noticed the same behaviour for $L/D \leq 1.0$.

The middle graph of Fig. 9 shows the dominant frequency signature of the response. The plain cylinder follows the typical frequency behaviour expected for 1-dof VIV, following the dotdashed line indicating St=0.2 and slightly departing from the natural frequency during the synchronisation range. The cylinder fitted with fixed devices, on the other hand, adopts much lower frequencies of vibration, not related to the vortex shedding mechanism. In addition, the bottom graph of Fig. 9 reveals no drag amplification for the suppressors through the synchronisation range would be expected if they were vibrating due to VIV. The steep ramp in the displacement curve, the low-frequency signature and no amplification of drag are all evidence that the system is indeed being driven by a 1-dof galloping mechanism. In fact, Assi et al. (2009) showed that the origin of the lift force causing galloping is that of the mean lift that appears for free-torotate devices with an angular deflection.

Flow visualisation and PIV measurements were carried out to investigate the interaction between the wake and the fixed devices. Figs. 10–12 present instantaneous vorticity fields for three different reduced velocities of 3.0, 5.0 and 7.3, identified with a (*) in the axis of Fig. 9 (top) for convenience. The data was acquired when the cylinder was crossing the centreline from left to right, therefore presenting maximum cross-flow velocity; flow direction is from top to bottom. A key for colour contours is not presented in these figures because the objective is only the qualitative comparison of the wake.

Fig. 10 presents vorticity contours of the wake of a plain cylinder under VIV for reference. For reduced velocity 3.0 in Fig. 10(a) the cylinder presents small vibration with a typical 2S-mode wake being shed (refer to Williamson and Govardhan, 2004 for a description of wake modes). For reduced velocity 5.0 in Fig. 10(b), close to the peak of resonance, the wake appears much wider due to the high-amplitude movement of the cylinder. The wake mode will change again in the lower branch of vibration as it appears for reduced velocity 7.3 in Fig. 10(c). For all cases in Fig. 10 the interaction of the separated shear layers in the vortex-formation mechanism is quite evident.

Figs. 11 and 12 present vorticity contours for a cylinder fitted with non-rotating splitter plates of lengths L/D=0.5 and 1.0, respectively. For both plate lengths and for almost all reduced velocities the shear layer that separates from the right-hand side of the cylinder reattaches to the tip of the plate. An exception is the short plate at reduced velocity 3.0 in Fig. 11(a), where the vortices are able to form downstream of the plate without any reattachment. As explained in Assi et al. (2009), the reattachment of the shear layer on the right-hand side will create a lift force towards that side, which is in phase with the velocity of the cylinder. This galloping excitation is observed to occur for both plate lengths. Although one may think that the 1D-long plate would be able to extract more energy from the flow during the galloping mechanism, the response of both plates in Fig. 9 (top) is rather similar.

An identical galloping mechanism appears to occur with the non-rotating short-tail fairing, as presented in Fig. 13. For reduced velocity 3.0 in Fig. 13(a) the vortex shedding mechanism is not affected by the presence of the fairing in quite the same way the

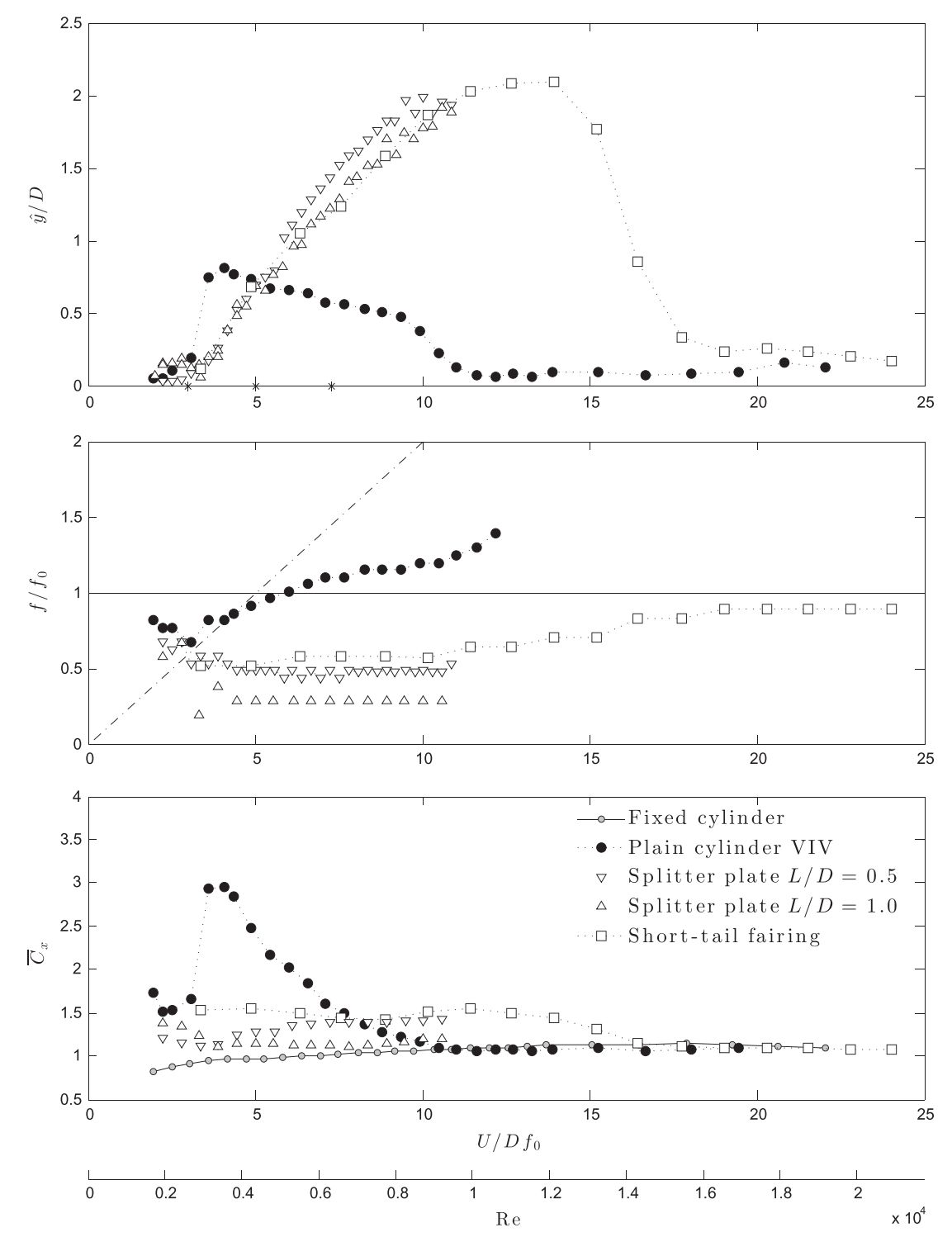


Fig. 9. 1-dof galloping response of cylinder fitted with non-rotating devices. Displacement (top) and frequency (middle) of vibration and mean drag coefficient (bottom) versus reduced velocity.

short plate is unnoticed by the flow in Fig. 11(a). As reduced velocity (and Reynolds number) is increased the vortex formation length is reduced and the reattachment of the shear layer due to the relative motion of the fairing is achieved. All three cases illustrated in Fig. 13 are essentially identical to those for the short plate in Fig. 11. In fact, the responses of these short suppressors are not at all different, as seen in Fig. 9. We believe this explains how a non-rotating short-tail fairing can undergo galloping instabilities in the same way as a splitter plate with equivalent characteristic length. Again, Fig. 8 summarises the idea that the origin of the

steady lift on a free-to-rotate but deflected suppressor is the same as that to cause galloping in a non-rotating fairing.

Once the devices were allowed to rotate about the centre of the cylinder the 1-dof responses were completely different. The plates and the fairing tilted to an inclined position and the low-amplitude levels of displacement proved that they successfully suppressed VIV. The previous work of Assi et al. (2009) showed that rotary inertia is not an important parameter for stability, at least not as important as rotary friction (in the form of rotary damping). Marine growth, for example, would certainly affect

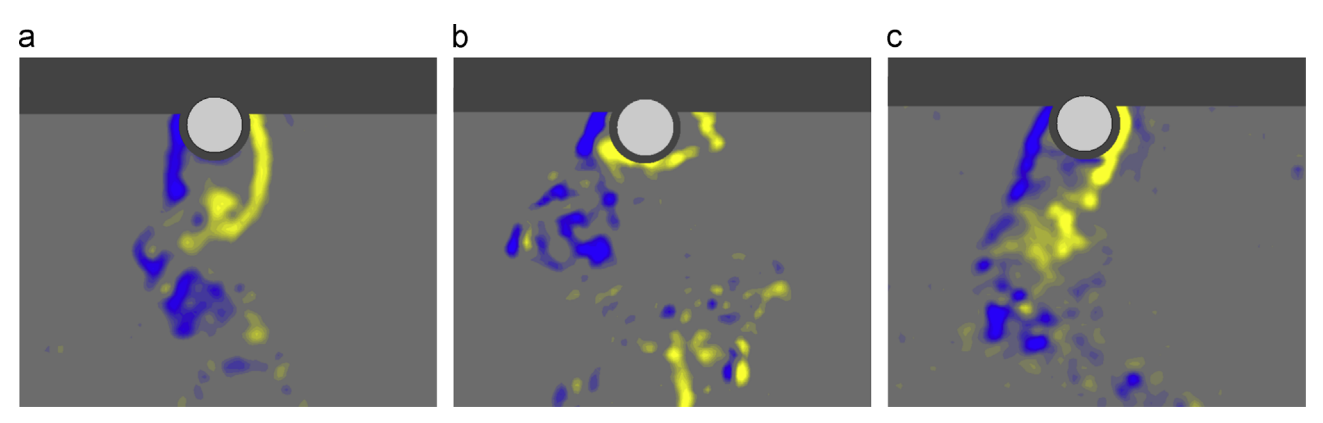


Fig. 10. Vorticity contours for a single cylinder. (a) $U/Df_0 = 3.0$; (b) $U/Df_0 = 5.0$; (c) $U/Df_0 = 7.3$. (For interpretation of the references to color in this figure legend, the reader is referred to the web version of this article.)

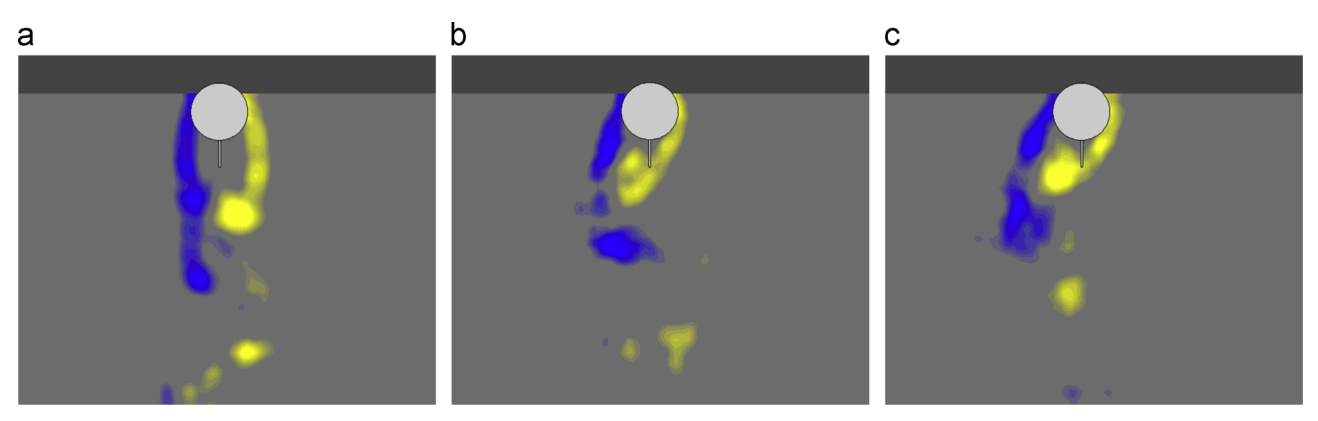


Fig. 11. Vorticity contours for a non-rotating splitter plate L/D = 0.5. (a) $U/Df_0 = 3.0$; (b) $U/Df_0 = 5.0$; (c) $U/Df_0 = 7.3$. (For interpretation of the references to color in this figure legend, the reader is referred to the web version of this article.)

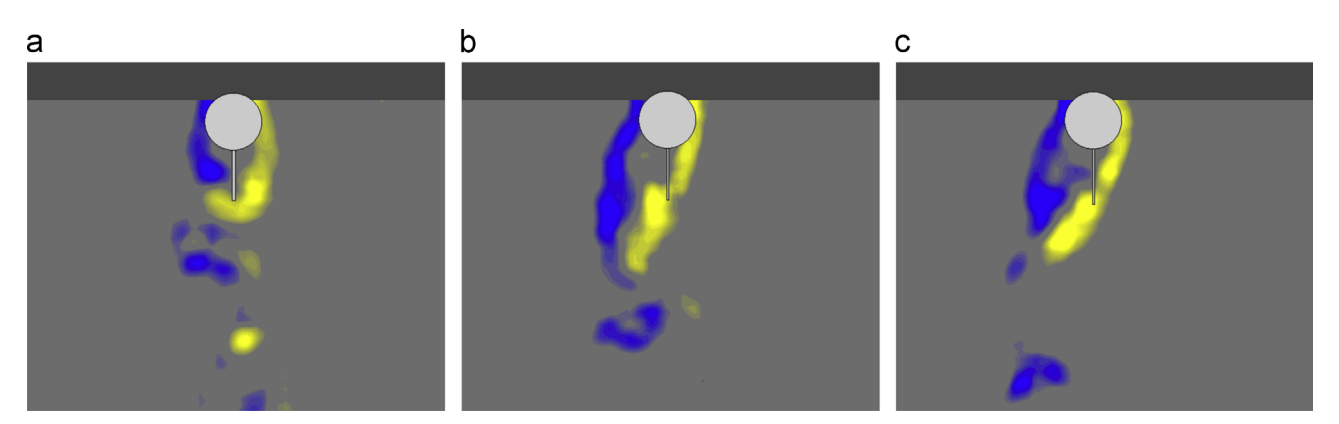


Fig. 12. Vorticity contours for a non-rotating splitter plate L/D = 1.0. (a) $U/Df_0 = 3.0$; (b) $U/Df_0 = 5.0$; (c) $U/Df_0 = 7.3$. (For interpretation of the references to color in this figure legend, the reader is referred to the web version of this article.)

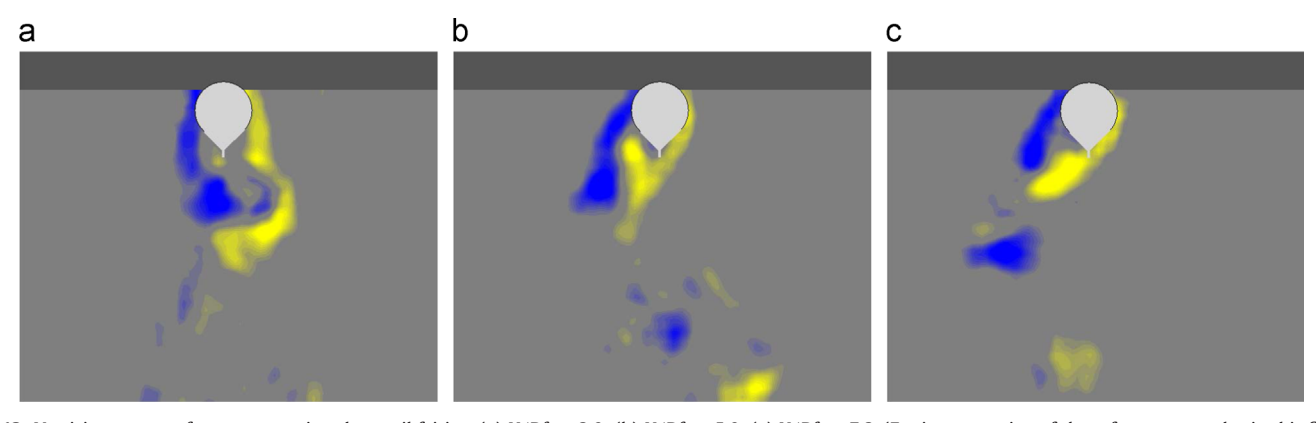


Fig. 13. Vorticity contours for a non-rotating short-tail fairing. (a) $U/Df_0 = 3.0$; (b) $U/Df_0 = 5.0$; (c) $U/Df_0 = 7.3$. (For interpretation of the references to color in this figure legend, the reader is referred to the web version of this article.)

rotary friction, thus altering the stability of the system. Although fairings are being used to suppress VIV in practical offshore applications, our results show that a non-rotating fairing (for example, a fairing that got stuck) can cause severe galloping over a considerable range of flow speeds.

5. Conclusions

Following this study we have achieved a better understanding of the hydroelastic principles behind the way short-tail fairings work to reduce VIV. It appears that the short-tail fairing behaves in a similar manner to a single splitter plate of equivalent characteristic length.

Although the critical value of rotational friction has not been determined for a short-tail fairing, our results suggests that a critical value exists between the low and the high friction cases presented here. It seems likely that different suppressors might have different stability boundaries for rotational resistance, but there is clearly a range of τ_f within which VIV suppression would be achieved with short-tail fairings.

Short-tail fairings with a characteristic length of 0.5D proved to reduce amplitude levels (at the expense of a mean transverse force) but were not as efficient as other longer suppressors reported in Assi et al. (2009). Rather than reducing drag for the entire range of reduced velocities tested, the fairing increased it for certain velocities. As a result, the average drag has a similar level to that of a plain fixed cylinder, offering a slight reduction of 6% throughout the Reynolds number range.

Non-rotating splitter plates produced severe galloping response in 1-dof, reaching the limiting amplitude for the apparatus $(\hat{y}/D=2)$ at reduced velocity 10. The non-rotating short-tail fairing presented similar behaviour, but an abrupt decrease in the response was observed for reduced velocity 14. PIV measurements revealed the behaviour of the flow inducing the galloping instability.

As with all circular cylinder flows, undoubtedly Reynolds number plays a role and hence some caution may need to be exercised in extrapolating the results presented here to full-scale risers. However, the underlying flow physics is not expected to change and the devices described in this study are likely to be effective at suppressing VIV when applied to full-scale risers.

Acknowledgements

The authors wish to acknowledge the support of BP Exploration Operating Company and BP America Production Company. GRSA is

grateful to the support of CAPES Brazilian Ministry of Education (2668-04-1) at the time of the experiments and acknowledges the support of FAPESP (2013/07335-8) and CNPq (308916/2012-3) that allowed him the time to revisit the data and prepare this paper.

References

- Allen, D.W., Henning, D., May 1995. Small fixed teardrop fairings for vortex induced vibration suppression. United States Patent (number 5.410.979).
- Assi, G.R.S., Bearman, P.W., Carmo, B., Meneghini, J., Sherwin, S., Willden, R., 2013a. The role of wake stiffness on the wake-induced vibration of the downstream cylinder of a tandem pair. J. Fluid Mech. 718, 210–245.
- Assi, G.R.S., Bearman, P.W., Kitney, N., 2009. Low drag solutions for suppressing vortex-induced vibration of circular cylinders. J. Fluids Struct. 25, 666–675.
- Assi, G.R.S., Bearman, P.W., Kitney, N., Tognarelli, M., 2010a. Suppression of wakeinduced vibration of tandem cylinders with free-to-rotate control plates. J. Fluids Struct. 26, 1045–1057.
- Assi, G.R.S., Bearman, P.W., Meneghini, J., 2010b. On the wake-induced vibration of tandem circular cylinders: the vortex interaction excitation mechanism. J. Fluid Mech. 661, 365–401.
- Assi, G.R.S., Franco, G.S., 2013. Experimental investigation on the stability of parallel and oblique plates as suppressors of vortex-induced vibration. In: Proceedings of OMAE2013, Thirty-second International Conference on Ocean, Offshore and Arctic Engineering, 2013, Nantes, France.
- Assi, G.R.S., Franco, G.S., Vestri, M.S., 2013b. Instability and Control of Massively Separated Flows. Springer (Ch. Notes on the stability of free-to-rotate plates suppressing the vortex-induced vibration of a circular cylinder).
- Assi, G.R.S., Rodrigues, J., Freire, C., 2012. The effect of plate length on the behaviour of free-to-rotate VIV suppressors with parallel plates. In: Proceedings of OMAE2012, Thirty-first International Conference on Ocean, Offshore and Arctic Engineering, Rio de Janeiro, Brazil.
- Brankovic, M., 2004. Vortex-induced Vibration Attenuation of Circular Cylinders with Low Mass and Damping (Ph.D. thesis). Imperial College, London, UK.
- Cimbala, J., Garg, S., 1991. Flow in the wake of a freely rotatable cylinder with splitter plate. AIAA J. 29, 1001–1003.
- Dahl, J., Hover, F., Triantafyllou, M., 2006. Two-degree-of-freedom vortex-induced vibrations using a force assisted apparatus. J. Fluids Struct. 22, 807–818.
- Every, M., King, R., Weaver, D., 1982. Vortex-excited vibrations of cylinders and cables and their suppression. Ocean Eng. 9 (2), 135–157.
- Henderson, J., 1978. Some towing problems with faired cables. Ocean Eng. 5, 105–125.
- Jauvtis, N., Williamson, C.H.K., 2004. The effect of two degrees of freedom on vortex-induced vibration at low mass and damping. J. Fluid Mech. 509, 23–62.
- Packwood, A., 1990. Performance of segmented swept and unswept cable fairings at low reynolds numbers. Ocean Eng. 17, 393–407.
- Pontaza, J., Chen, H., 2006. Numerical simulations of circular cylinders outfitted with vortex-induced vibrations suppressors. In: ISOPE Int. Soc. Offshore and Polar Eng.
- Stappenbelt, B., 2010. Splitter-plate wake stabilisation and low aspect ratio cylinder flow-induced vibration mitigation. Int. J. Offshore Polar Eng. 20 (3), 1–6.
- Williamson, C.H.K., Govardhan, R., 2004. Vortex-induced vibrations. Annu. Rev. Fluid Mech. 36, 413–455.
- Wingham, P., 1983. Comparative steady state deep towing performance of bare and faired cable systems. Ocean Eng. 10, 1–32.
- Zdravkovich, M.M., 1981. Review and classification of various aerodynamic and hydrodynamic means for suppressing vortex shedding. J. Wind Eng. Ind. Aerodyn, 7, 145–189.